



## Gut microbiota from colorectal cancer patients enhances the progression of intestinal adenoma in *Apc*<sup>min/+</sup> mice

Lu Li<sup>a,1</sup>, Xiaofei Li<sup>a,1</sup>, Weilong Zhong<sup>a,1</sup>, Min Yang<sup>a</sup>, Mengque Xu<sup>a,b</sup>, Yue Sun<sup>a</sup>, Jiaheng Ma<sup>a</sup>, Tianyu Liu<sup>a</sup>, Xueli Song<sup>a</sup>, Wenxiao Dong<sup>a</sup>, Xiang Liu<sup>a</sup>, Yange Chen<sup>a</sup>, Yi Liu<sup>c,d</sup>, Zariya Ablad<sup>d</sup>, Wentian Liu<sup>a</sup>, Bangmao Wang<sup>a,\*</sup>, Kui Jiang<sup>a,\*</sup>, Hailong Cao<sup>a,d,\*\*</sup>

<sup>a</sup> Department of Gastroenterology and Hepatology, General Hospital, Tianjin Medical University, Tianjin, China

<sup>b</sup> Department of Gastroenterology, Sir Run Run Shaw Hospital, School of Medicine, Zhejiang University, Hangzhou, China

<sup>c</sup> Department of Gastroenterology and Hepatology, Tianjin Third Central Hospital, Tianjin, China

<sup>d</sup> Department of Gastroenterology and Hepatology, Hotan District People's Hospital, Xinjiang Uygur Autonomous Region, Xinjiang, China

### ARTICLE INFO

#### Article history:

Received 24 July 2019

Revised 5 September 2019

Accepted 11 September 2019

Available online 5 October 2019

#### Keywords:

Colorectal cancer

Gut microbiota

Fecal microbiota transplantation

Wnt signalling pathway

*Apc*<sup>min/+</sup> mice

### ABSTRACT

**Background:** Accumulating evidence points to a close relationship between gut dysbiosis and colorectal cancer (CRC). As >90% of CRC develop from adenoma, we aimed to investigate the crucial role of imbalanced gut microbiota on the progression of intestinal adenoma.

**Methods:** The *Apc*<sup>min/+</sup> mice gavage with phosphate-buffered saline (PBS), feces from healthy controls or CRC patients after antibiotic cocktails. The intestinal tissues were isolated for histopathology, western blotting, and RNA-seq. The microbiota of feces and short-chain fatty acids (SCFAs) were analysed by 16S rDNA Amplicon Sequencing and gas chromatography.

**Findings:** The *Apc*<sup>min/+</sup> mice gavaged by feces from CRC patients had more intestinal tumours compared with those fed with feces from healthy controls or PBS. Administration of feces from CRC patients increased tumour proliferation and decreased apoptosis in tumour cells, accompanied by impairment of gut barrier function and up-regulation the pro-inflammatory cytokines profile. The up-regulated the expression of  $\beta$ -catenin and cyclinD1 further indicating the activation of Wnt signalling pathway. The abundance of pathogenic bacteria was increased after FMT, while producing SCFAs bacteria and SCFAs production were decreased.

**Interpretation:** Gut microbiota of CRC patients disrupted intestinal barrier, induced low-grade inflammation and dysbiosis. The altered gut microbiota enhanced the progression of intestinal adenomas in *Apc*<sup>min/+</sup> mice, suggesting that a new strategy to target gut microbiota against CRC could be noted.

**Fund:** The study was supported by the [National Natural Science Foundation of China](http://www.nsf.gov/), Tianjin Research Programme of Application Foundation and Advanced Technology of China, and [China Postdoctoral Science Foundation](http://www.cpsf.gov/).

© 2019 Published by Elsevier B.V.

This is an open access article under the CC BY-NC-ND license.

(<http://creativecommons.org/licenses/by-nc-nd/4.0/>)

\* Corresponding authors.

\*\* Corresponding author at: Department of Gastroenterology and Hepatology, General Hospital, Tianjin Medical University, 154 Anshan Road, Heping District, Tianjin 300052, China.

E-mail addresses: [tjmughji@hotmail.com](mailto:tjmughji@hotmail.com), [mwang02@tmu.edu.cn](mailto:mwang02@tmu.edu.cn) (B. Wang), [kjiang@tmu.edu.cn](mailto:kjiang@tmu.edu.cn) (K. Jiang), [caohailong@tmu.edu.cn](mailto:caohailong@tmu.edu.cn) (H. Cao).

<sup>1</sup> These authors have contributed equally to this work.

## Research in context

### Evidence before this study

Colorectal cancer (CRC) is the third most common cancer caused by genetic predisposition and environment factors. Recent studies have suggested that CRC correlated gut microbiota dysbiosis, but the mechanisms need to be further investigated.

### Added value of this study

We firstly investigated the role of gut microbiota in the progression of intestinal adenoma using the mouse model with *adenomatous polyposis coli* (*Apc*) gene mutation through fecal microbiota transplantation (FMT). In our study, gut microbiota from CRC patients accelerated the sequence of intestinal adenoma-adenocarcinoma in *Apc*<sup>min/+</sup> mice. At the same time, intestinal barrier disruption, chronic low-grade inflammation, activation of Wnt signalling pathway, and imbalance of gut microbiota were accompanied.

### Implications of all the available evidence

Our study provides the direct evidence for the promotion of adenoma progression reduced by gut microbiota from CRC patients, and offers a translational perspective against CRC.

## 1. Introduction

Colorectal cancer (CRC), which ranks third in morbidity and second highest mortality, is one of the most common malignancies both in China and elsewhere [1]. Risk factors of CRC including genetic predisposition and environmental factors such as age, gender, obesity, chronic inflammation, lifestyle, physical activity, sedentary behaviour, and diet [2–4]. The pathogenesis of CRC, either intrinsic or acquired, is multifactorial and multistep [5,6]. Accumulating evidence suggests that the gut microbiota, chronic inflammation, host genetic predisposition, and environmental factors have been linked with the progression of CRC [7]. About 95% of intestinal tumours develop from adenomas [8], however its mechanisms have not been fully elucidated.

A large number of microorganisms, including bacteria, fungi, and viruses, colonize the gut and maintain a dynamic balance. Intestinal microorganisms are involved in the digestion and absorption of food, which can also enhance the intestinal defence function and promote the maturation of the immune system [9–11]. When the balance is broken, the disturbed intestinal microbial community will cause a variety of diseases, including CRC [12,13]. Emerging studies have found significant differences in intestinal microbial communities between CRC patients and healthy individuals [14]. CRC is closely related to intestinal dysbiosis [15–17]. *Fusobacterium nucleatum*, *Enterococcus faecalis*, *Bacteroides fragilis*, and *Escherichia coli*, etc were found to be enriched in the feces of CRC patients and to promote the occurrence of CRC [18]. Current studies suggest that imbalanced intestinal microbial communities contribute to the development of CRC partly due to by inducing chronic inflammation, activating regulatory T cells to trigger the immune response, releasing cytotoxins, and synthesizing and secreting metabolite products [19–21]. Interestingly, the fecal samples of CRC patients can induce intestinal tumorigenesis and colon cell proliferation in colon tumour model mice induced by chemical carcinogen azomethane oxide (AOM), as well as increase the expression of inflammatory genes and carcinogenic factors and infil-

tration of immune cells in AOM-induced mice and Germ-free mice [22]. However, the role of gut microbiota on adenoma progression in the *Apc* gene knockout (*Apc*<sup>min/+</sup>) model has not been investigated.

It is worth exploring the relationship between dysbiosis and adenoma progression. Therefore, we proposed the hypothesis that gut microbiota from CRC patients promoted the progression of intestinal adenomas in *Apc*<sup>min/+</sup> mice. The *Apc*<sup>min/+</sup> mice can spontaneously develop multiple intestinal adenomas with or without low-grade dysplasia. Therefore, it is an appropriate animal model for the study of intestinal tumours. Adenomatous polyposis coli (*Apc*) is a recognized key tumour suppressor gene in CRC, and its mutation is an early event of adenoma formation [23]. In our study, gut microbiota of CRC patients was transplanted into *Apc*<sup>min/+</sup> mice to explore the role of gut microbiota imbalance in the progression of intestinal adenoma under the background of genetic factors. We found the gut microbiota from CRC patients promoted adenoma progression, impaired function of the intestinal barrier, induced chronic low-grade inflammation, and activated Wnt signalling pathway. Thus, microbial targeted therapy may be a novel therapeutic strategy for CRC patients.

## 2. Materials and methods

### 2.1. Participants

Eligible patients diagnosed as CRC by colonoscopy at the Endoscopy Centre at the Department of Gastroenterology and Hepatology, General Hospital, Tianjin Medical University, China were enrolled in the study. The exclusion criteria of patient were as follows [22,24]: A history of antibiotic or probiotics treatment during the 3 months preceding fecal samples collected; A history of other types of gastrointestinal cancer or colitis-associated diseases; Diverticulosis or diverticulitis; A history of atopic or autoimmune diseases or ongoing immunomodulatory therapy; A history of neurological or neurodevelopmental disorders or of chronic pain syndromes; Obesity (BMI >30 kg/m<sup>2</sup>), metabolic syndrome or moderate to severe malnutrition; A history of malignant diseases or ongoing oncologic therapy; Vegetarian; A history of fecal microbiota transplantation.

Healthy controls were recruited from asymptomatic volunteers who underwent colonoscopy with no significant abnormalities. The exclusion criteria were consistent with CRC patients. All Subjects information was provided in the Table 1. All donors have undergone rigorous screening and underwent informed consent for stool donation. The human study conformed “International ethical guidelines for biomedical research involving human subjects (2002)” developed by Council For International Organizations Of Medical Sciences (CIOMS) in collaboration with World Health Organization (WHO), which was approved by the ethics committee of General Hospital of Tianjin Medical University.

### 2.2. Animals and study design

The twenty conventional female C57BL/6J mice (4 weeks of age) were obtained from Beijing Animal Study Centre, and thirty *Apc*<sup>min/+</sup> mice aged 4 weeks on C57BL/6J background were purchased from Animal Model Institution of Nanjing University, P. R. China. All mice were maintained in specific pathogen free (SPF) condition of experimental animal centre of Tianjin Medical University, and kept in strict accordance with the operating procedures. AIN-93M rodent diet and sterilized water were provided *ad libitum* throughout the experiment. Mice were acclimatized a 12:12 light-dark cycle.

After receiving antibiotic cocktails mixed by 200 mg/L ampicillin, metronidazole, neomycin and 100 mg/L of vancomycin in

**Table 1**  
Clinical characteristics of the human donors for stool gavage to mice.

Group	Age (years)	Sex	BMI (kg/m <sup>2</sup> )	CRC stage	TNM stage	Site of tumour	Family history of CRC	Smoking	Drinking	Dietary preference
Healthy control	53	Male	22.37	N	N	N	N	Y	Y	Normal diet
	54	Female	18.59	N	N	N	N	N	N	Normal diet
	56	Female	19.47	N	N	N	N	N	N	Sweet food
	58	Female	20.07	N	N	N	N	N	N	Normal diet
	60	Male	23.12	N	N	N	N	N	N	Normal diet
	63	Male	21.56	N	N	N	N	N	N	Normal diet
	66	Male	20.57	N	N	N	N	N	N	Normal diet
	67	Female	22.09	N	N	N	N	Y	N	Spicy food
	70	Male	22.25	N	N	N	N	N	N	Normal diet
	72	Female	23.84	N	N	N	N	N	N	Normal diet
CRC cases	49	Female	21.34	IIIb	T3N1M0	Sigmoid	N	N	N	Normal diet
	55	Female	19.86	Ila	T3N0M0	Sigmoid	N	Y	Y	Normal diet
	58	Male	20.13	IIIb	T3N1M0	Rectum	N	Y	Y	Normal diet
	61	Male	20.49	IIIb	T3N1M0	Rectum	N	Y	N	Normal diet
	68	Female	21.45	IIIa	T2N1M0	Rectum	N	N	N	Sweet food
	68	Male	20.02	IIIa	T2N1M0	Sigmoid	N	Y	Y	Normal diet
	69	Male	19.38	Ila	T3N0M0	Sigmoid	N	N	Y	Spicy food
	73	Male	24.86	Ila	T3N0M0	Sigmoid	N	N	N	Sweet food
	74	Male	21.31	IIIa	T2N1M0	Sigmoid	N	N	N	Sweet food
	82	Female	19.54	IIIb	T3N1M0	Sigmoid	Y	N	N	Sweet food

CRC: Colorectal cancer; BMI: Body Mass Index; Y, Yes; N, NO.

drinking water for three days according to the previous studies [22], all mice were randomly divided into five groups with 10 mice each. The C57BL/6J mice were divided into two groups: One group was gavaged fecal samples from healthy controls (FMT-CH), while the other group was gavaged fecal samples from patients with CRC (FMT-CC). The *Apc*<sup>min/+</sup> mice were divided into three groups: PBS group (gavage of phosphate-buffered saline), FMT-AH group (gavage of fecal samples from healthy controls) and FMT-AC group (gavage of fecal samples from patients with CRC). The animal use protocol has been reviewed and approved by the Animal Ethical and Welfare Committee (AEWC) of Tianjin Medical University.

### 2.3. Fecal microbiota transplantation (FMT)

After two weeks of colonoscopy, participants were informed to collect fecal samples with sterile containers and the samples were stored at -80 °C as soon as processed. Fecal samples from 10 patients with CRC(CRC) and 10 healthy controls (Control) were mixed at equal weight, respectively. One gram of the mixed feces was diluted in 5 mL sterile PBS solution, then initial filtered, concentrated, homogenized, step by step filtered, centrifuged. The supernatant was collected, isolated, purified and equally repackaged before kept in -80 °C refrigerator [25–27].

The fecal microbiota transplantation (FMT) was repeated 16 times during the experimental period of 8 weeks after pre-treatment with antibiotics, the mice were gavaged once a day during the first week, and three times a week in the second week. For the next 6 weeks, the mice were administered once a week (Fig. 1a). A volume of 200 μL suspension was gavaged to each mouse each time [28–30]. Each group of mice used a separate set of intragastric apparatus.

### 2.4. Tissue collection and histopathology

The mice were sacrificed under anaesthesia after FMT. The whole intestine was isolated and rinsed with ice-cold sterile PBS solution. The small intestine was divided into proximal, middle and distal segments on average, with the colorectum as the fourth segment. Intestinal tumour burden was recorded according to its intestinal site and maximum diameter by an Olympus SZX7 stereo dissecting microscope. The tumour burden was based on gross counts. The proximal tissue of each intestinal segment was snap frozen in liquid nitrogen and kept at -80 °C later and the distal tissue was fixed with 4% paraformaldehyde.

Paraffin-embedded intestinal tissue was cut into 5 μm slices for H&E staining. Pathological types of specimens were diagnosed by two experienced pathologists who were unaware of the treatment allocation of the mice.

### 2.5. Immunohistochemistry staining

Paraffin-embedded intestinal tissue cut into 5-μm slices by a microtome were also subjected to immunostaining for detecting the expressions of Ki-67 (Abcam Cat# ab16667, RRID: AB\_302459), lysozyme (Abcam Cat# ab108508, RRID:AB\_10861277), β-catenin (Abcam Cat# ab32572, RRID:AB\_725966), and cyclin D1 (Abcam Cat# ab16663, RRID:AB\_443423). Intestinal tissues were dewaxed with xylene, rehydrated in graded ethanol, and treated with 3% hydrogen peroxide to abolish endogenous peroxidase activity. Slices were thermally repaired with sodium citrate buffer and incubated with corresponding primary antibody at 4 °C overnight. The Slices were restored to room temperature the next day and incubated with second antibody for 30 min at 37 °C. Then, Slices went through DAB reaction, washing, haematoxylin red dyeing, dehydration and drying sequentially.

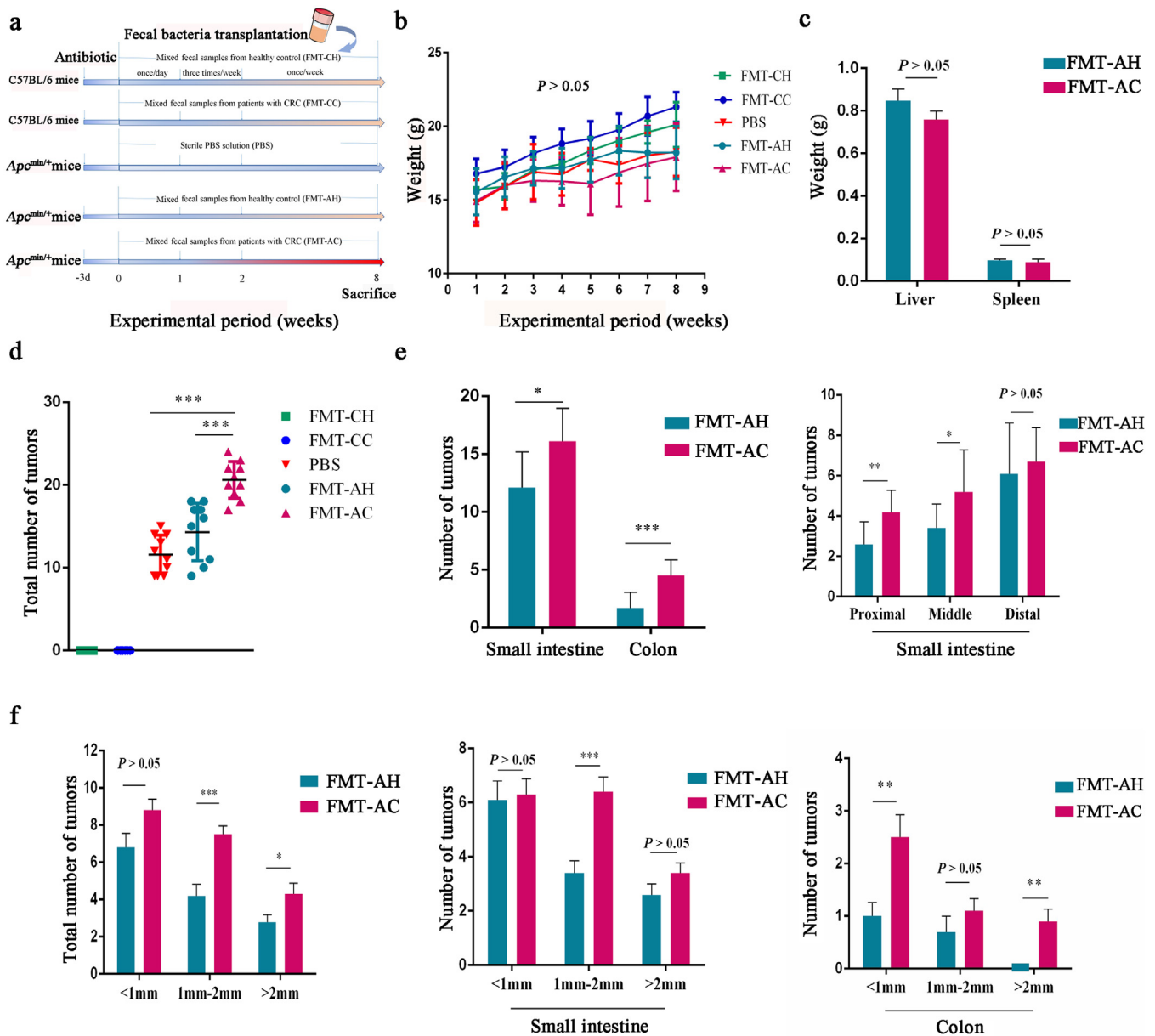


**Fig. 1.** Gut Microbiota from colorectal cancer patients increased intestinal tumours in *Apc<sup>min/+</sup>* mice. (a) The treatment process of fecal microbiota transplantation (FMT) during 8 weeks. (b) Body weight of each group was recorded weekly. (c) Comparison of liver and spleen weight between FMT-AH group and FMT-AC group. (d) Total number of tumours in each group. (e) The number of tumours in the small intestine and colon between the FMT-AH group and the FMT-AC group. (f) The total number of tumours, small intestinal, and colon tumours were calculated according to the diameter. Data are expressed as means  $\pm$  SEM. FMT-AH, gavage of fecal samples from healthy controls ( $n = 10$ ). FMT-AC, gavage of fecal samples from colorectal cancer patients ( $n = 10$ ). \*  $p < .05$ , \*\*  $p < .01$ , \*\*\*  $p < .001$ .

Under normal conditions,  $\beta$ -catenin expression was localized in the cell membrane, with continuous brown-yellow staining along the cell membrane. Ectopic expression occurs when the cytoplasm and nucleus appear brownish yellow, and cells with ectopic expression are defined as positive cells. The normal expression of cyclin D1 was in the nucleus, and the brown-yellow colour of the stained nucleus was the positive cell [31]. Five areas randomly selected from each section were viewed at the tumour tissue. The percentage of positive cells in each field was calculated by Image J.

## 2.6. Immunofluorescence and TUNEL assay

Paraffin sections were immersed in xylene and gradient concentration ethanol for dewaxing, incubated at room temperature for 10 min with 3% hydrogen peroxide, followed by citrate for antigen thermal repair, sealed with 5% goat serum for 20 min, and incu-

bated with primary antibody IgA (ab223410, Abcam, rabbit, anti-mouse, 1:100) at 4°C overnight. The slices were restored to room temperature the next day and incubated with goat anti-rabbit containing FITC for 1 h at 37°C. Then, Slices went through DAPI reaction, sealed, observed under fluorescence microscope.

Terminal deoxynucleotidyl transferase dUTP nick end labelling (TUNEL) was used to detect tumour cellular apoptosis. The instructions for *in situ* cell apoptosis detection kit were followed, and the treated sections were photographed by fluorescence microscope. The FITC- labelled green areas were considered positive cells and were analysed using the Image J.

## 2.7. Periodic acid-Schiff (PAS) staining

Colon sections were incubated with 1% periodic acid solution (Sigma-Aldrich) for 10 min, and with Schiff reagent (Sigma-Aldrich)

**Table 2**  
The Oligonucleotide primers used in Realtime-PCR analysis.

Murine gene	Primer sequences
GAPDH	Forward primer: 5'-TGTGTCCGTCGTGGATCTGA-3' Reverse primer: 5'-CTGCTTACCACCTTCTTGA-3'
ZO-1	Forward primer: 5'-GGGCATCTCAACTCTGTA-3' Reverse primer: 5'-AGAAGGGCTGACGGGTAAT-3'
Claudin 3	Forward primer: 5'-CTGTGGATGAAGTGGTG-3' Reverse primer: 5'-GTAGTCTTGGGTCGTAG-3'
Occludin	Forward primer: 5'-ACTATGCGGAAAGAGTTGACAG-3' Reverse primer: 5'-GTCATCCACACTCAAGGTCAG-3'
Muc2	Forward primer: 5'-TCGCCAAGTCGACACTCA-3' Reverse primer: 5'-GCAAATAGCCATAGTACAGTTACACAGC-3'
Cryptdin	Forward primer: 5'-CAGCCGGAGAAGAGGACCAG-3' Reverse primer: 5'-TAGCATACCAGATCTCTCAACGATTC-3'
Reg3 $\gamma$	Forward primer: 5'-TTCCTGTCTCCATGATCAAAA-3' Reverse primer: 5'-CATCCACCTCTGTGGGTTCA-3'
NLRP3	Forward primer: 5'-CTCCAACCATTCTGACCAG-3' Reverse primer: 5'-ACAGATTGAAGTAAGCGCG-3'
IL-1 $\beta$	Forward primer: 5'-GTGGCTGTGGAGAAGCTGTG-3' Reverse primer: 5'-GAAGTCCACGGGAAAGACAC-3'
TNF- $\alpha$	Forward primer: 5'-ACTCCAGGCGTGCCTATG-3' Reverse primer: 5'-GAGCGTGGTGGCCCT-3'

for 40 min subsequently, and followed by haematoxylin dye for 5 min.

### 2.8. RNA extraction and Realtime-PCR

Total RNA was extracted using the RNeasy mini kit, and cDNA reverse transcription was carried out using the TIAN Script RT Kit according to the manufacturer's instructions. The oligonucleotide primers for target genes were shown in Table 2. The relative mRNA expression was performed using a standard  $\Delta\Delta$ CT method to calculate fold-changes normalized to housekeeping genes for each sample.

### 2.9. RNA-seq

After the RNA sample from small intestinal tumour tissues of FMT-AH and FMT-AC groups were qualified, mRNA was enriched with magnetic beads with Oligo (dT). cDNA was synthesized using mRNA fragmented into short fragments by fragmentation buffer. Qubit 2.0 was used for preliminary quantification. The qualified libraries were sequenced on a HiSeq X-Ten (Illumina). NGS QC Toolkit (v2.3.3) was used to filter data, and the TopHat (v2.0.13) was used to perform the alignment.

In order to make the gene expression levels between different treatment comparable, expected number of fragments per kilobase of transcript sequence per million base pairs sequenced (FPKM) was used to standardize the gene expression quantity. Analysis of differentially expressed genes was performed using the Noisseq package. Genes with folding changes >2 and probability >.8 were defined as differentially expressed genes. Then, GO function was used to analysed the functional classification annotation and functional significance enrichment of differentially expressed genes. GO analysis were performed used the software of Clue GO, plugin of CytoScape. Blast2GO (v2.5.0) was used to obtain the Gene Ontology (GO) annotation information of Unigene.

### 2.10. Western blotting

Intestinal tumour tissue was adequately homogenized on ice in a mixture of RIPA, PMSF, and protease inhibitors. Centrifugation was spun at 13000 rpm to collect the supernatant containing total protein. The instructions of Nuclear and Cytoplasmic Protein Extraction Kit were strictly performed in order to extract nuclear protein. The protein concentration was determined

using the Bicinchoninic acid protein assay kit (Thermo Scientific Inc) to achieve equal loading in the subsequent experiments. After adding a certain volume of loading buffer, the protein samples were boiled for 10 min, loaded and resolved on 12% SDS-PAGE gels, transferred to a nitrocellulose filter membrane, blocked with 5% milk or bovine serum albumin, and incubated in primary antibodies at 4 °C overnight followed by secondary antibodies for 2 h at room temperature. The primary anti- $\beta$ -catenin (rabbit, anti-mouse, ab32572, Abcam, 1:5000), anti-cyclin D1 (rabbit, anti-mouse, ab16663, Abcam, 1:10000), anti-c-myc (rabbit, anti-mouse, Cat#ab32072, Abcam, 1:1000, RRID:AB\_731658), anti- $\beta$ -actin(mouse, Cat#mAb3700, CST, 1:1000, RRID:AB\_2128511), anti-histone 2A (rabbit, anti-mouse, Cat# ab124781, Abcam, 1:1000, RRID:AB\_10971675) antibody were applied. Secondary antibodies were horseradish peroxidase conjugated anti-rabbit or anti-mouse. Chemiluminescence signals were detected by the ECL detection kit. The intensity of Western blotting images was determined by Image J.

### 2.11. 16S rDNA amplicon sequencing

Fresh feces of *Apc*<sup>min/+</sup> mice after FMT were collected for 16S rDNA Amplicon sequencing which was performed by the Re-albio Genomics Institute (Shanghai, China). After genomic DNA extraction by QIAamp® Fast DNA Stool Mini Kit (QIAamp, Germany), Thermo Nano Drop 2000 uv microspectrophotometer and 1% agarose gel electrophoresis were used for quality control. Specific primers (341 F: 5'-ACTCCTACGGGRCAGCAG-3', 806 R: 5'-GGACTACVVGGGTATCTAATC-3') were used for PCR amplification and product purification using the KAPA HiFi Hotstart Ready Mix PCR kit. Qubit was used for quantitative and homogenization after the library was constructed and passed the quality inspection. The libraries were sequenced using Illumina HiSeq PE250. After the removal of chimeric sequences by Userach (v7.0.1090), Operational Taxonomic Units (OTU<sub>S</sub>) were picked at a standard clustering with 97% similarity using UPARSE. Each representative tag was assigned to a taxa by RDP Classifier against the RDP database using confidence threshold of 0.8. According to the number of sequences in each OTU, OTUs abundance tables are obtained for subsequent analysis. OTU profiling table, alpha/beta diversity and rank abundance curve analyses were implemented by QIIME1 (v1.9.1). Lefse (v1.0) and rank sum test (R version 3.5.1) were used to screen different species and different functions.

### 2.12. Determination of short-chain fatty acids in cecal contents

The concentrations of SCFAs (acetate, propionate and butyrate) in cecal contents were measured by gas chromatography (GC). Briefly after the appropriate sample was shaken with 3 mL HCL (1 mol/L), ultrasound was performed for 10 min in an ice bath. The supernatant was centrifuged at 12000 rpm for 15 min. A volume of 1 mL supernatant was added to 1 mL ethyl acetate for extraction. Then the supernatant was centrifuged at 12000 rpm for 15 min again. After pre-treatment, the samples were equipped to a HP-INNOWAX capillary column for chromatographic separation. Column flow rate was maintained at 2 mL/min. The temperature was first increased at a rate of 20 °C/min to 150 °C. Then, the temperature was increased to 180 °C at a rate of 5 °C/min for 1 min.

### 2.13. Statistical analysis and Data accession

Data were expressed as mean  $\pm$  standard deviation. Statistical analysis between two groups was performed using the Student's *t*-test. Differences among more than two groups were tested by one-way ANOVA. The pathological characteristics of both cohorts

were performed by chi-squared tests.  $P < .05$  was considered significant. Statistical analysis was performed on SPSS 22.0. The RNA-seq data was stored in Gene Expression Omnibus (GEO) database: GSE136682. The 16S rDNA Amplicon Sequencing data was deposited in Sequence Read Archive (SRA) database: PRJNA563239.

### 3. Results

#### 3.1. FMT tolerance

The body weight of mice in each group increased slowly (Fig. 1b), but it did not differ significantly among groups ( $P > .05$ ). Over the eight weeks period, all mice were well tolerated and survive after FMT. After FMT for eight weeks, two mice in the FMT-AH group, and six mice in the FMT-AC group presented diarrhoea and bloody stools ( $P > .05$ ). No significant gross bloody stool was observed in the PBS group. In addition, the weight of the liver and spleen was similar in the FMT-AC group compared to the FMT-AH group (Fig. 1c).

#### 3.2. Gut microbiota from CRC patients aggravated the progression of intestinal adenoma

The impact of FMT on intestinal adenoma was evaluated at week eight. No tumour was found in FMT-CH group or FMT-CC group. The burden of intestinal adenomas in PBS group and FMT-AH group did not differ significantly. The total number of adenomas in mice receiving fecal samples from CRC patients was increased compared with the PBS group, and the mice receiving fecal samples from healthy controls ( $F(2,27) = 28.67, P < .01$ ) (Fig. 1d). The number of adenomas were increased mainly in the proximal and middle of the small intestine than that in the FMT-AH group. However, there was no significant difference in the distal small intestine (Fig. 1e).

The number of intestinal adenomas in mice was calculated according to the maximum diameter  $< 1$  mm, 1–2 mm, and  $> 2$  mm, respectively. The total number of adenomas with diameter of 1–2 mm and  $> 2$  mm in the FMT-AC group was increased than that in the FMT-AH group (1–2 mm:  $7.50 \pm 0.45$  vs  $4.20 \pm 0.63, P < .001$ ;  $> 2$  mm:  $4.30 \pm 0.59$  vs  $2.80 \pm 0.39, P = .04$ ). The number of small intestinal adenomas with the diameter of 1–2 mm in the FMT-AC group was significantly increased ( $6.40 \pm 0.54$  vs  $3.40 \pm 0.45, P < .001$ ). The number of colorectal adenomas in the FMT-AC group was ( $0.90 \pm 0.23$ ). However, there were no adenomas with a maximum diameter of  $> 2$  mm in the FMT-AH group ( $P = .0012$ ) (Fig. 1f).

In the PBS group and FMT-AH group, a few scattered small polyps were observed, while more tumours were observed in the FMT-AC group, especially the large polyps protruding into the lumen appeared in the colon (Fig. 2a). A total of 7 mice harboured high-grade dysplasia in the FMT-AC group ( $7/10 = 70.0\%$ ), while only 1 mouse showed high-grade dysplasia ( $1/10 = 10.0\%$ ) ( $P = .02$ ) (Fig. 2b). Gut Microbiota from CRC patients promoted the progression of intestinal adenoma in *Apc*<sup>min/+</sup> mice.

To explore the effect of gut microbiota from CRC on tumour cells, we detected the proliferation and apoptosis in intestinal tumour tissues. The rate of Ki-67 positive cells in FMT-AC group was significantly increased than that in FMT-AH group ( $75.40 \pm 3.16$  vs  $43.40 \pm 3.52, P < .001$ ). Compared with the FMT-AH group, the number of apoptotic cells decreased in the FMT-AC group (Fig. 2c). Therefore, the results suggested that gut microbiota from CRC patients promoted proliferation and inhibited apoptosis in intestinal tumours cells.

#### 3.3. Gut microbiota from CRC patients impaired intestinal barrier function

Next, we evaluated the intestinal barrier function which an important defence system against pathogens in mice after FMT. The mRNA expression of tight junction proteins, including ZO-1, Occludin, and Claudin3 decreased after FMT from CRC patients (Fig. 3a).

PAS staining of colon tissues revealed that the average number of goblet cells in each crypt was lower in the FMT-AC group. Immunohistochemical showed that lysozyme positive cells were significantly reduced in the FMT-AC group (Fig. 3b). The gut microbiota from CRC patients down-regulated the mRNA expression of Muc2 which is the main component of the mucus layer indicating the secretory function was impaired. Cryptdin and regenerating islet-derived protein (Reg3 $\gamma$ ) are the antimicrobial peptides secreted by Paneth cells, which protects the intestine from infection by enteropathogenic bacteria. The mRNA expression of Cryptdin and Reg3 $\gamma$  also decreased (Fig. 3c). These data showed gut microbiota from CRC patients impaired Goblet cells and Paneth cells.

Intestinal secretory immunoglobulin A (sIgA) is a major immune effector molecule on the gastrointestinal mucosa, which is an important defence line against pathogenic mucosal adhesion and colonization. The expression of sIgA were decreased in the mice receiving fecal samples from CRC patients (Fig. 3d). These results indicated that not limited to mechanical barriers, chemical and immune barriers were also impaired.

#### 3.4. Gut microbiota from CRC patients induced chronic low-grade inflammation

Chronic inflammation is a recognized risk factor for CRC [32]. In our study, no significant inflammatory cell infiltration was observed under the microscope in the intestinal tissues of mice in all groups by HE staining. However, Realtime-PCR showed the expression of pro-inflammatory cytokines including NOD-like receptor family, pyrin domain containing 3 (NLRP3), Interleukin-1 $\beta$  (IL-1 $\beta$ ), and Tumour necrosis factor- $\alpha$  (TNF- $\alpha$ ) were up-regulated in FMT-AC group (Fig. 3a). It suggested the gut microbiota from CRC patients induced chronic low-grade inflammation in *Apc*<sup>min/+</sup> mice.

#### 3.5. Differentially expressed genes in intestinal tumour tissues after FMT

We performed RNA-Seq analysis to obtain global transcriptomic profiles of tumour tissues. RNA sequencing revealed genes differentially expressed after FMT. Hierarchical clustering analysis was carried out according to FPKM of each sample, and the mice of FMT-AH group clustered with FMT-AH group and the mice of FMT-AC group clustered with FMT-AC group (Fig. 4a). Compared with the FMT-AH group, we obtained 228 up-regulated and 50 down-regulated genes in the FMT-AC group (Fig. 4b). GO analyses of up-regulated genes showed enriched “Wnt-protein binding”, “Lipid metabolic process” and “T-helper 17 type immune response” pathways, respectively. Activation of the Wnt signalling pathway, abnormal lipid metabolism, and the immune system play critical roles in the progression of adenomas (Fig. 4c and d). The RNA-seq transcriptome study was contributed to illustrate gene pathways relevant to Wnt signalling pathway, and provided us with clues to further study.

#### 3.6. Gut microbiota from CRC patients activated Wnt signalling pathway

The expression of  $\beta$ -catenin in the FMT-AH group was mainly located in the cell membrane. However, the gut microbiota from

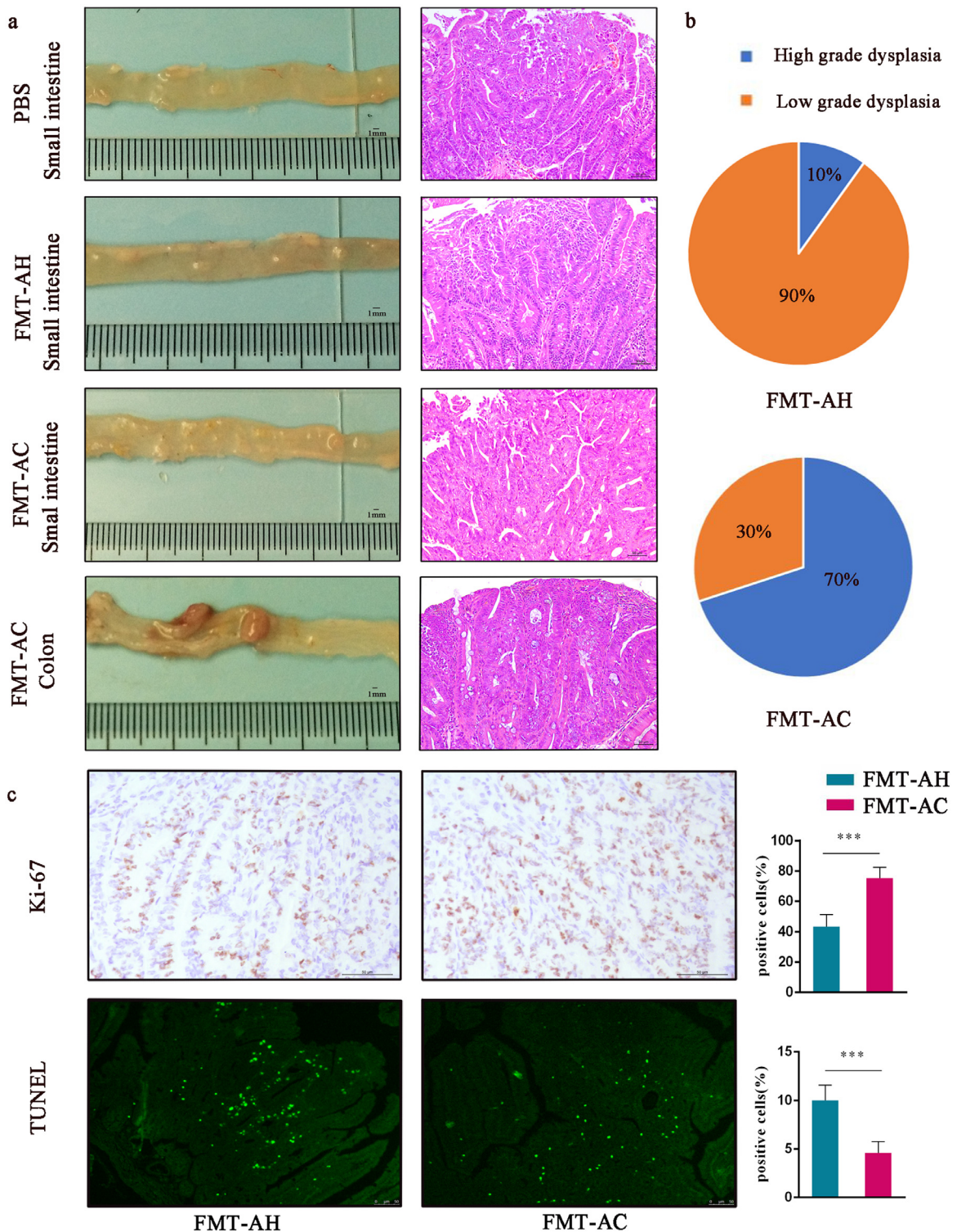


**Fig. 2.** Gut microbiota from colorectal cancer patients enhanced the progression of intestinal adenoma in *Apc*<sup>min/+</sup> mice. (a) Representative macroscopic images and HE staining of intestinal and tumours in three groups. (b) The proportion of malignant transformation in FMT-AH group and FMT-AC group. (c) Ki-67 and TUNEL staining in the small intestinal tumours. Five tumours tissues were randomly selected from each section to calculate the percentage of positive cells. Scale bars: 50  $\mu$ m. FMT-AH, gavage of fecal samples from healthy controls ( $n=10$ ). FMT-AC, gavage of fecal samples from colorectal cancer patients ( $n=10$ ).  $p=.02$ , \*\*\*  $p<.001$ .

CRC patients altered localization of  $\beta$ -catenin which promotes the transformation of cell membrane into cytoplasm and nucleus. Compared with the FMT-AH group, the percentage of cyclinD1 positive cells in the FMT-AC group significantly increased (Fig. 5a). Although there was no difference in total

$\beta$ -catenin protein expression, the protein level of active  $\beta$ -catenin, cyclinD1, and c-myc was increased in FMT-AC group (Fig. 5b). Taken together, the results suggest that the gut microbiota from CRC patients promoted activation of Wnt signalling pathway.

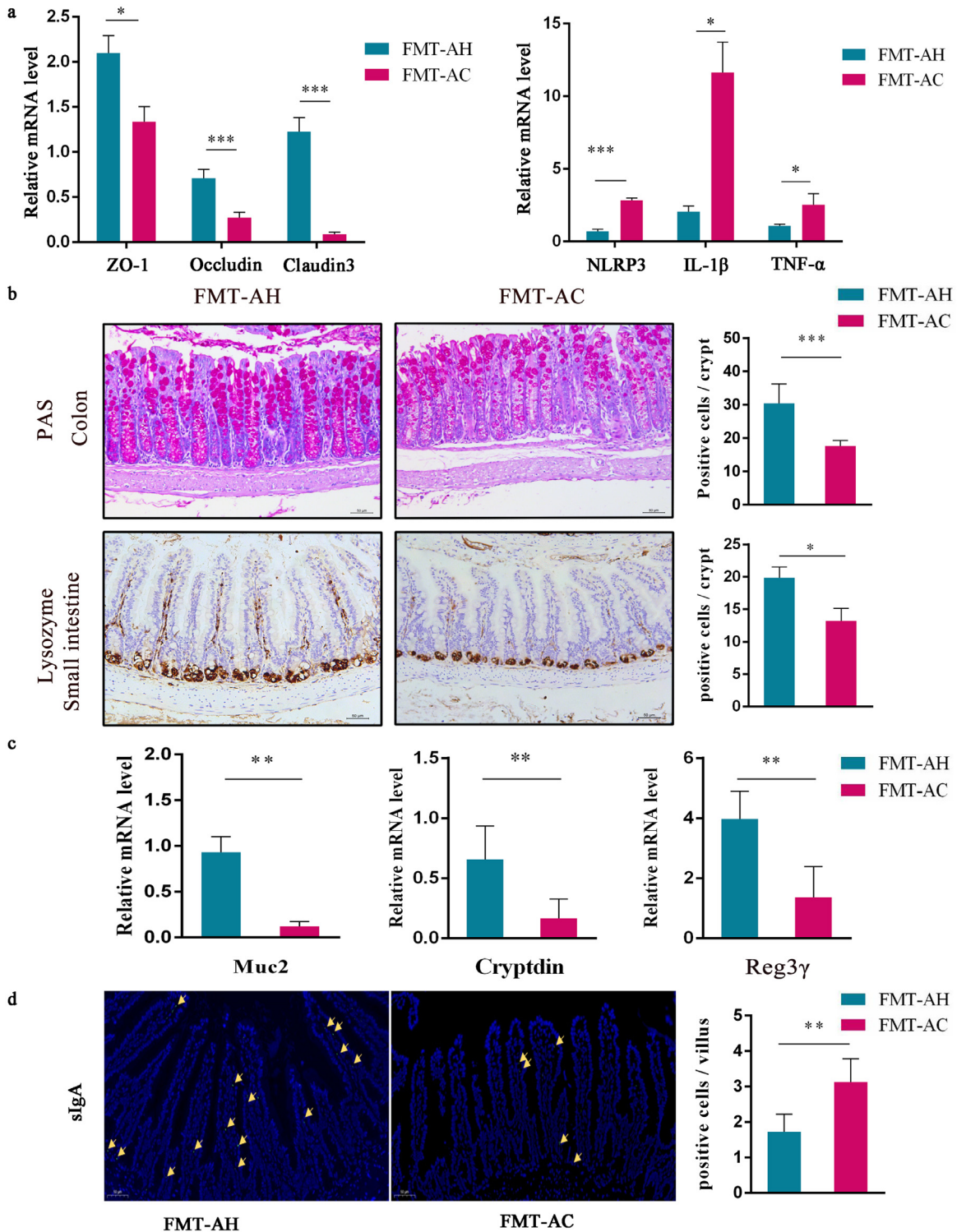


**Fig. 3.** Gut microbiota from colorectal cancer patients impaired the intestinal barrier and induced low grade inflammation in *Apc<sup>min/+</sup>* mice. (a) The relative mRNA level of ZO-1, Occludin, and Claudin3 was decreased in the small intestine tumours of the FMT-AC group and the relative mRNA level of NLRP3, IL-1 $\beta$ , and TNF- $\alpha$  was increased. (b) The number of colon goblet cells was evaluated by PAS staining. The number of Paneth cells in small intestine was evaluated by Lysozyme immunohistochemical staining. Five tissues were randomly selected from each section to calculate the percentage of positive cells per crypt. (c) The relative mRNA level of Muc2, Cryptdin, and Reg3 $\gamma$  was decreased in the FMT-AC group. (d) The expression of sIgA analysed by immunofluorescence. Scale bars: 50  $\mu$ m. FMT-AH, gavage of fecal samples from healthy controls (n = 10). FMT-AC, gavage of fecal samples from colorectal cancer patients (n = 10). \*  $p < .05$ , \*\*  $p < .01$ , \*\*\*  $p < .001$ .

### 3.7. Gut microbiota transmission after FMT

The components of the supernatant from different donors were detected. Compared with mixed fecal supernatant from healthy controls, the relative abundance of *Roseburia* and *Clostridium* in the

mixed fecal supernatant from CRC patients decreased at the genus level. Meanwhile, the relative abundance of *Akkermansia* increased (Fig. 6a).

Fresh fecal from mice were collected for detecting after the last FMT. The bacterial abundance was also different between the two



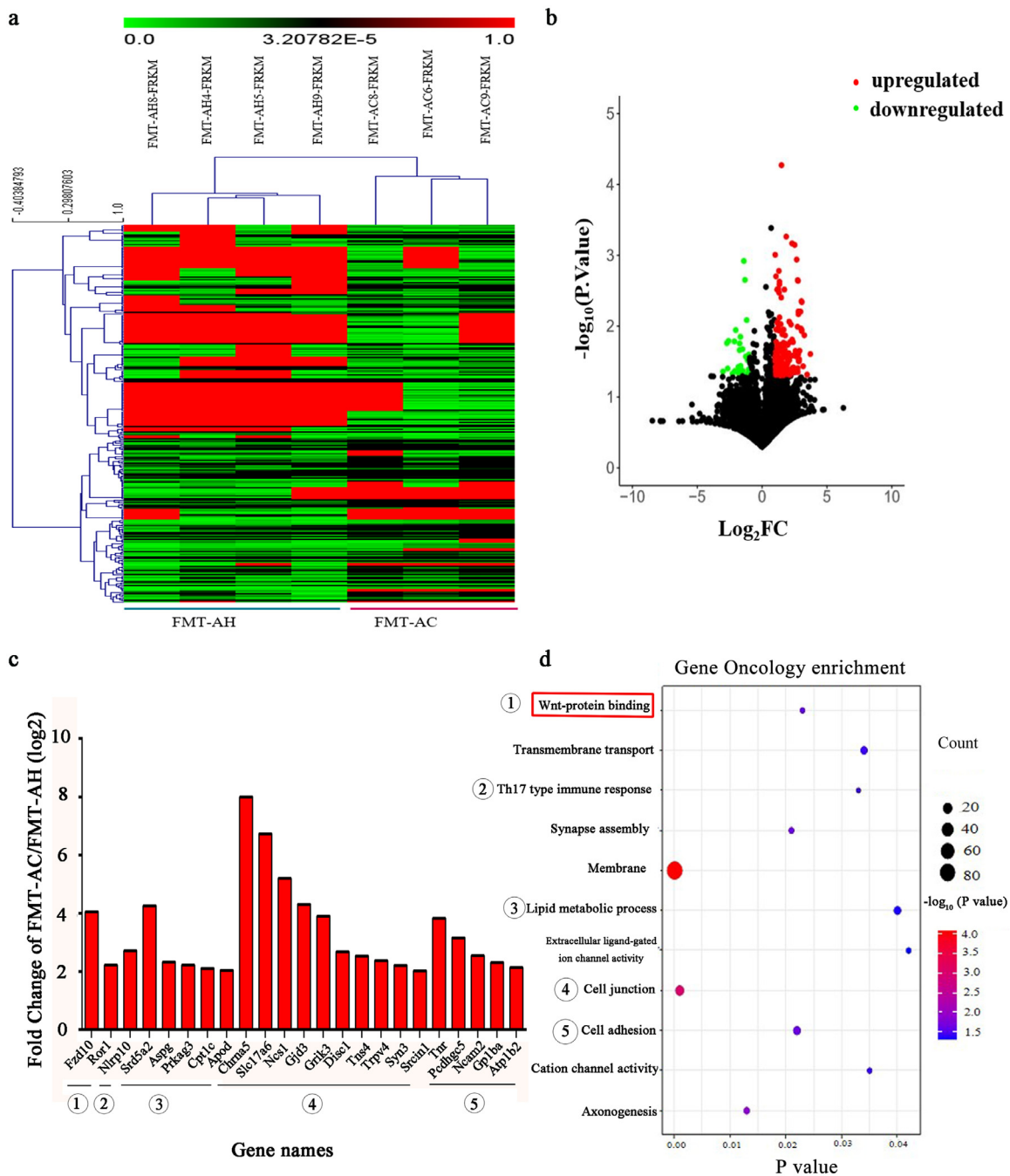


**Fig. 4.** Differentially expressed genes in intestinal tumour tissues. (a) Hierarchical clustering analysis was carried out according to expected number of fragments per kilobase of transcript sequence per million base pairs sequenced (FPKM) of samples. (b) FMT-AC group induced up-regulated and down-regulated genes compared with FMT-AH group. (c) Up-regulated gene enrichment function. (d) GO function annotation was carried out for differential genes. FMT-AH, gavage of fecal samples from healthy controls (n = 10). FMT-AC, gavage of fecal samples from colorectal cancer patients (n = 10).

groups at the genus level (Fig. 6b). There was no difference in  $\alpha$ -diversity between the two groups, the Simpson index and Shannon index shown in Fig. 6c and d. The MDS2 and ANOSIM's analysis representing the  $\beta$  diversity between the two groups showed significant differences (Fig. 6e and f). More importantly, the abundance of *Akkermansia* and *Pseudoflavonifractor* increased in FMT-AC group, which were significantly increased compared to the FMT-AH group. The levels of opportunistic pathogens, including *Prevotella*, *Escherichia coli* and *Helicobacter* increased in FMT-AC group. In contrast, the abundance of short-chain fatty acids (SCFAs) producing bacteria, such as *Ruminococcus*, *Roseburia* and *Clostridium XIVa*, were significantly lower (Fig. 7a and b). Next, we explored the

interactions between the communities. It suggests a negative relationship between *Roseburia* and *Eubacterium*. Similarly, *Flavonifractor* has an inverse relationship with *Bifidobacterium*. There exists an obvious positive relationship between *Anaerotruncus* and *Flavonifractor*, while a positive relationship between *Akkermansia* and *Phascolarctobacterium* was established (Fig. 7c).

We performed the correlation analysis between differentially expressed genes and bacterial abundance. The mice which gavaged by the fecal samples from healthy controls (FMT-AH) had enrichment of *Roseburia*, *Anaerotruncus*, *Flavonifractor*, and *Eisenbergiella*, while the mice which gavaged by the fecal samples from CRC patients (FMT-AC) had enrichment of *Eubacterium*; *Rikenella*,

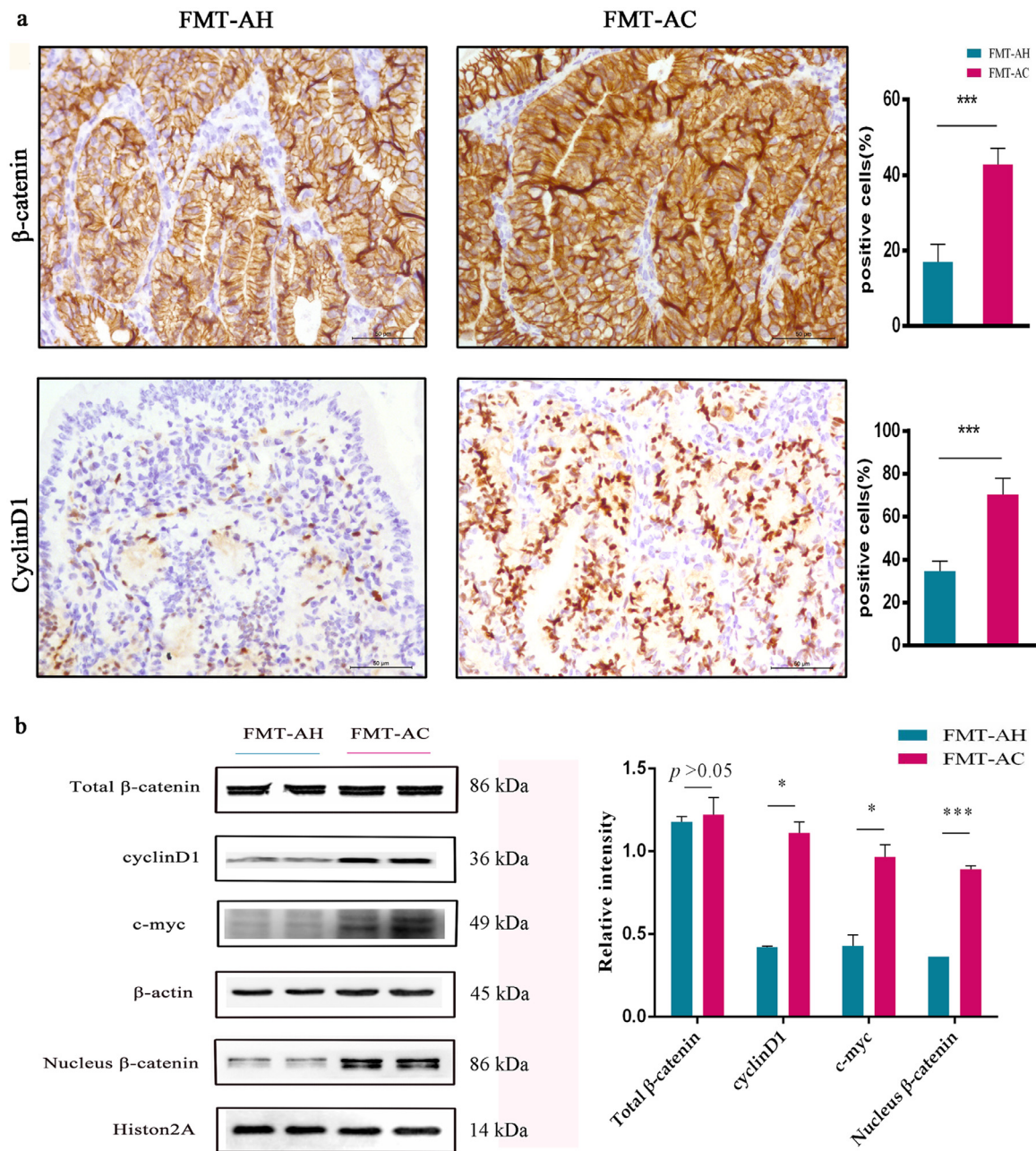


**Fig. 5.** Gut microbiota from colorectal cancer patients activated Wnt signalling pathway. (a)  $\beta$ -catenin and cyclinD1 in the small intestine tumours were assessed by immunostaining. (b) Protein levels of total  $\beta$ -catenin, cyclinD1, c-myc, and nucleus  $\beta$ -catenin in the small intestine tumours were detected by western blotting and the relative intensity was quantified. Scale bars: 50  $\mu$ m. FMT-AH, gavage of fecal samples from healthy controls (n = 10), FMT-AC, gavage of fecal samples from colorectal cancer patients (n = 10). \*  $p < .05$ , \*\*\*  $p < .001$ .

*Alistipes*, *Helicobacter* and *Bifidobacterium*. Interestingly, it is noteworthy that *Eubacterium* and *Roseburia* have significant correlation with the up-regulated differential genes. *Eubacterium* was negatively correlated with the expression of *Fzd10* and *Cpt1c*, while *Roseburia* was positively relevant with *Apod*, *Scd3*, *Tns4*, *Tdgl1*, etc. Others enriched bacteria, including *Anaerotruncus*, *Flavonifractor*, *Eisenbergiella*, *Rikenella*, *Alistipes*, showed no significant correlations with the up-regulated differential genes (Fig. 7d).

### 3.8. Gut microbiota from CRC patients decreased caecal concentrations of SCFAs

Gut microbiota-derived SCFAs have been certified to maintain intestinal homeostasis by protecting the integrity of epithelial bar-

rier [33] and regulating T-cell differentiation [34]. Microbial analysis of mice feces above revealed a decrease in the bacterial abundance in the FMT-AC group. Accordingly, we detected the content of acetate, propionate, and butyrate in cecum, which were reduced in the FMT-AC group compared to the FMT-AH group (Fig. 7e).

## 4. Discussion

In recent years, studies have revealed that gut microbiota dysbiosis is a crucial factor in the occurrence and development of CRC [35,36]. It seems to be accepted that CRC may be a bacterial related disease with a multistep from intestinal adenoma-adenocarcinoma sequence [5,37]. The present study demonstrated the effect and underlying mechanisms of the gut microbiota from

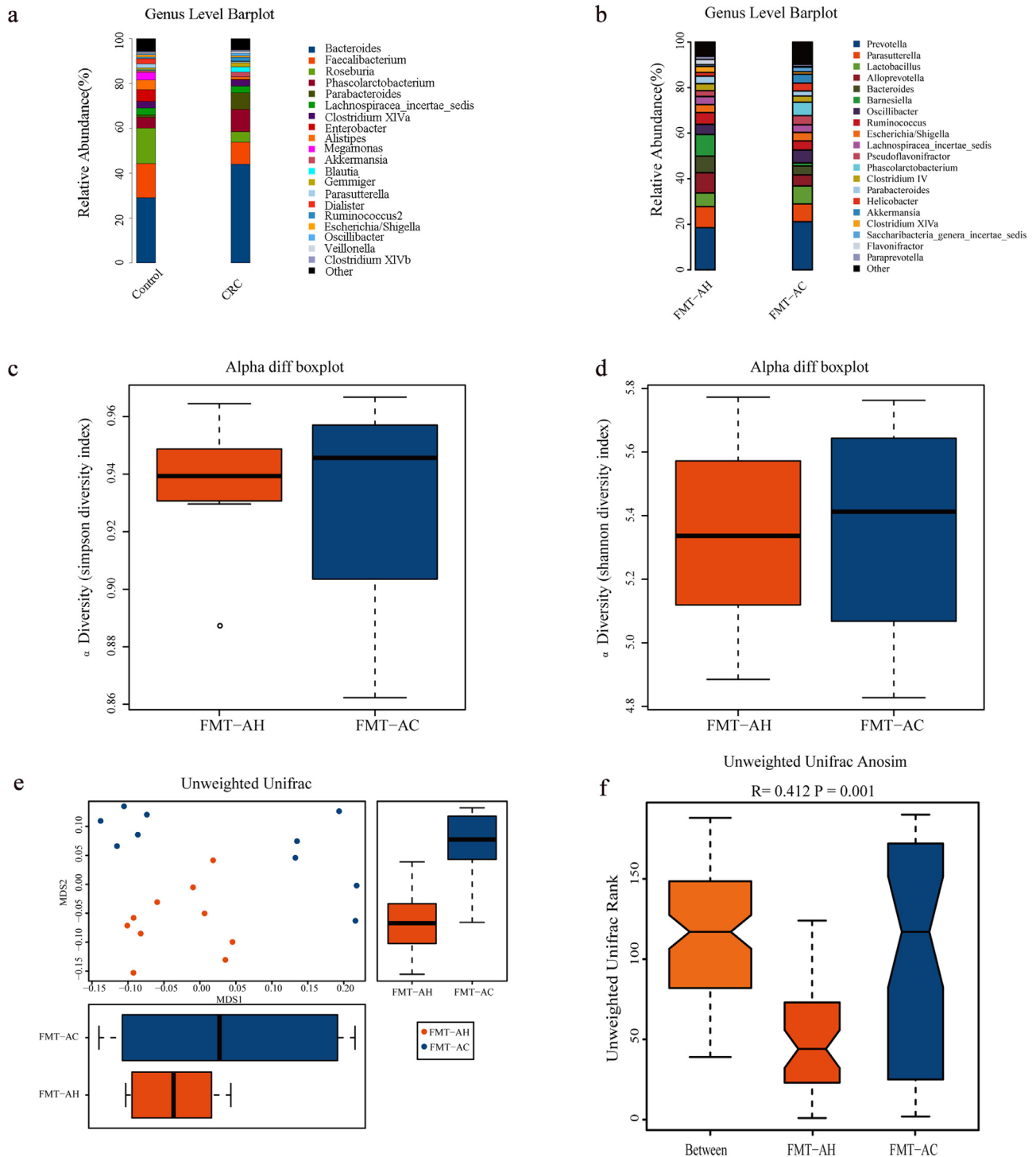


**Fig. 6.** Gut microbiota dysbiosis could be transmitted during intestinal adenoma progression. (a) The relative abundance of bacterial at genus levels between the control group and CRC group. (b) The relative abundance of bacterial at genus levels between the FMT-AH group and FMT-AC group. (c and d) The Simpson and Shannon index representing  $\alpha$  diversity between the two groups ( $P > .05$ ). (e and f) The MDS2 and ANOSIM's analysis representing the  $\beta$  diversity between the FMT-AH group and FMT-AC group ( $R = 0.412$ ,  $P = .001$ ). Control, mixed fecal samples from healthy controls ( $n = 10$ ). CRC, mixed fecal samples from colorectal cancer patients ( $n = 10$ ). FMT-AH, gavage of fecal samples from healthy controls ( $n = 10$ ). FMT-AC, gavage of fecal samples from colorectal cancer patients ( $n = 10$ ).

CRC on the progression of intestinal adenomas. We found that *Apc*<sup>min/+</sup> mice transplanted with gut microbiota from CRC patients showed intestinal mucosal barrier damage, low grade intestinal inflammation, activation of Wnt pathway and progression of adenomas (Fig. 8).

A balanced intestinal environment requires the cooperation of the host mucosal barrier and the immune system [38]. Transmem-

brane barrier proteins including claudins, occludin, JAM-A, which are closely linked with surrounding scaffold proteins such as ZO-1 and afadin are significant components of the intercellular barrier [39]. In addition to the physical barrier, intestinal epithelial cells also secrete mucus (goblet cells) and antimicrobial peptides (Paneth cells) that promote intestinal health [38]. Studies have shown that impaired intestinal barrier is conducive to bacterial

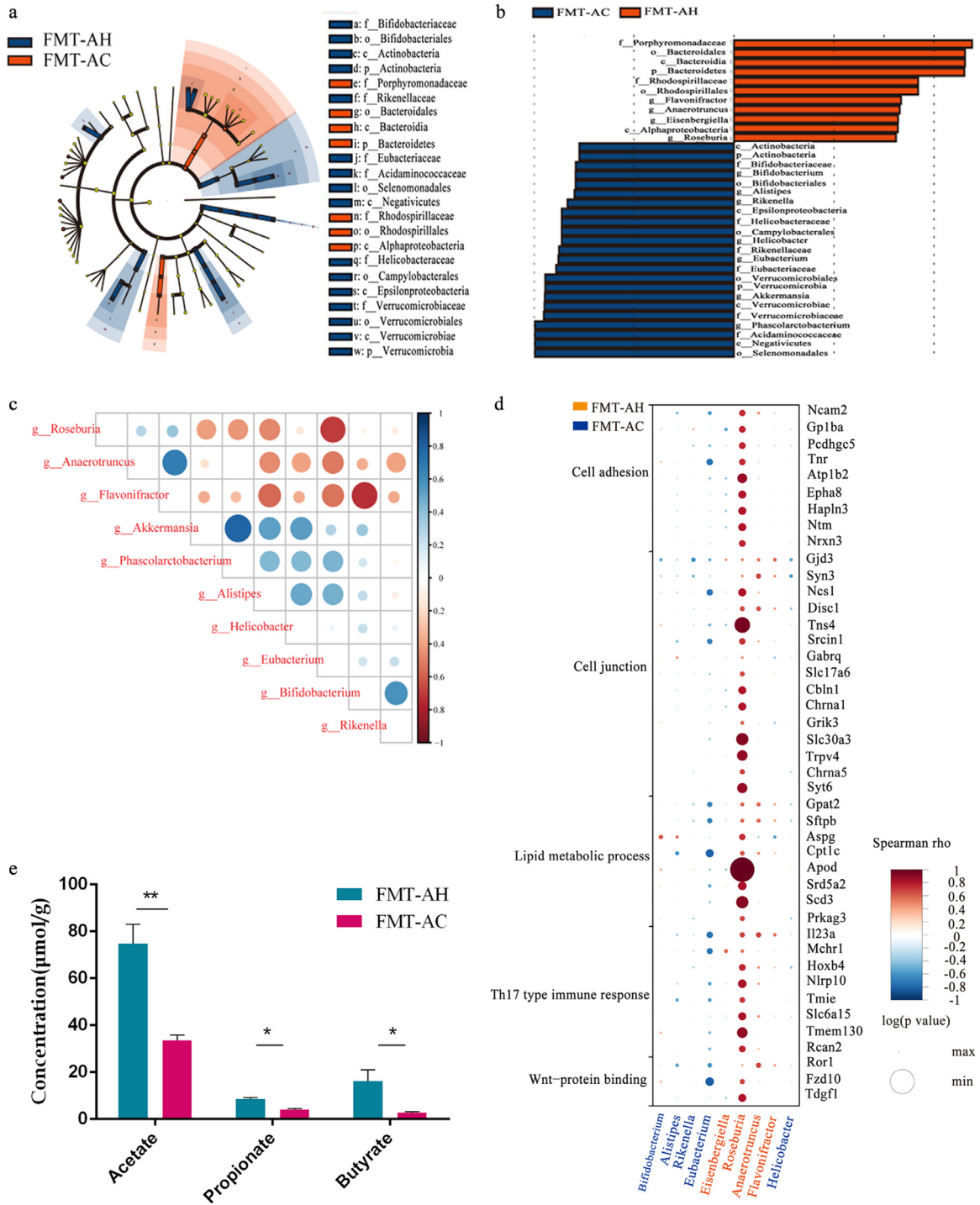


**Fig. 7.** The fecal microbial community alteration after fecal microbiota transplantation. (a and b) The significantly different bacteria between the FMT-AH group and FMT-AC group. (c) The correlation between different bacteria. (d) The correlation analysis between differential expressed genes and bacterial abundance. (e) The concentration of acetate, propionate, and butyrate was detected. FMT-AH, gavage of fecal samples from healthy people ( $n = 10$ ). FMT-AC, gavage of fecal samples from colorectal cancer patients ( $n = 10$ ). \*  $p < .05$ , \*\*  $p < .01$ .

ectopic and colonization, aggravating the inflammation and promoting the development of CRC [21]. Similarly, gut microbiota from CRC may effectively reduce the number and secretory products of Goblet and Paneth cells, and break the integrity of the intestinal barrier in our study.

It has been reported that *APC* is a canonical tumour suppressor gene in the development of colorectal cancer. The *Apc*<sup>min/+</sup> mice can spontaneously develop benign adenomatous polyps from

dysplastic crypts which surrounded by proliferative villi and crypts [40]. The burden of intestinal adenoma in *Apc*<sup>min/+</sup> mice increased with age. At the same time, along with low-grade intestinal inflammation, the disruption of intestinal barrier and the increased pathogenic bacteria also contributed to diarrhoea and gross bloody stool in *Apc*<sup>min/+</sup> mice, especially in the group which gavage of fecal samples from patients with CRC. Some research found that chronic inflammation was closely related to CRC. Current studies

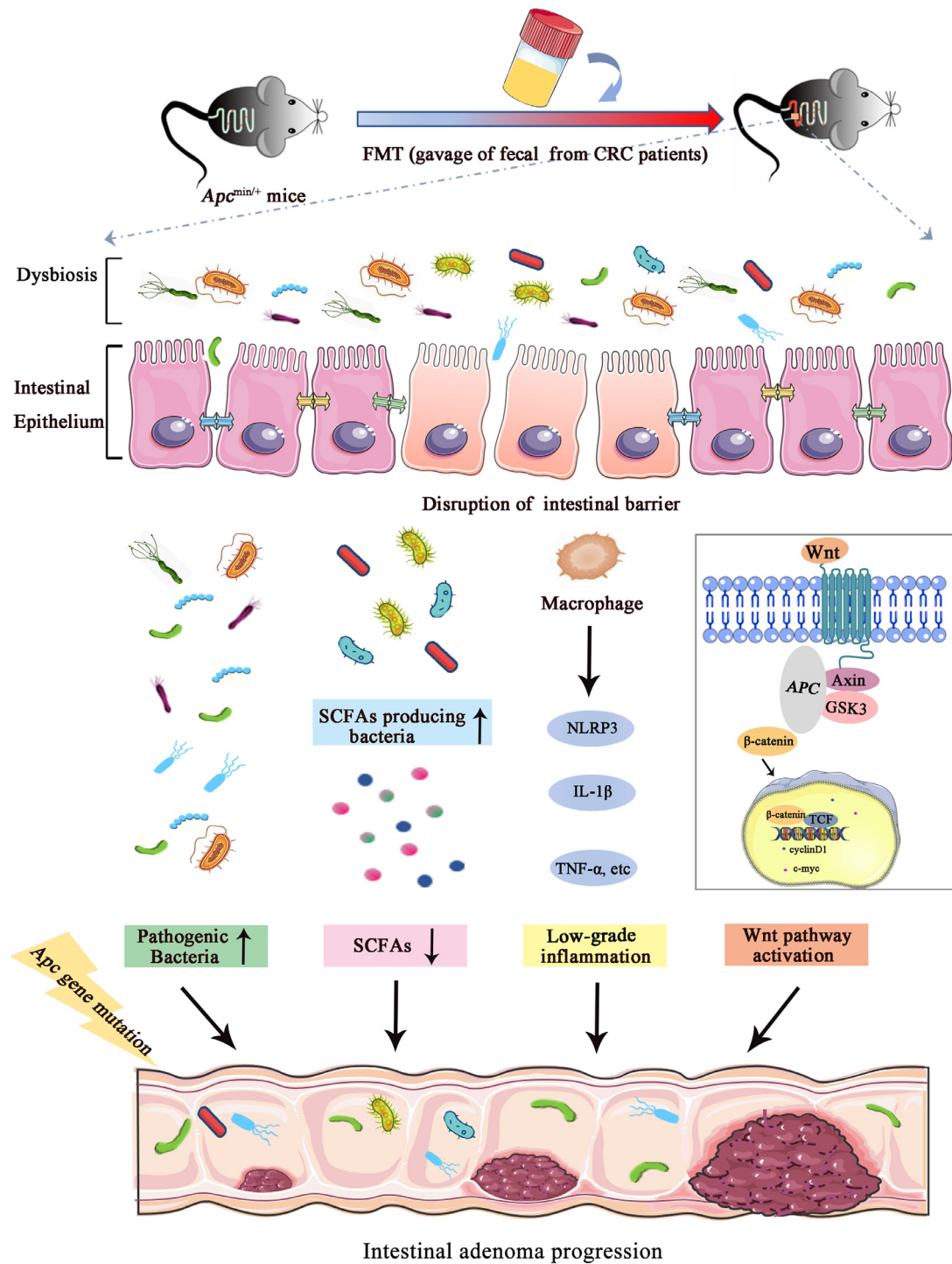


**Fig. 8.** Gut microbiota from colorectal cancer patients enhanced the progression of intestinal adenoma in *Apc<sup>min/+</sup>* mice. Gut microbiota from colorectal cancer patients disrupted the intestinal barrier, induced chronic low-grade inflammation, and active the Wnt signalling pathway. The abundance of pathogenic bacteria increased, while the abundance of SCFAs producing bacteria and SCFAs production decreased. Gut microbiota from CRC patients accelerated the progression of intestinal adenomas in *Apc<sup>min/+</sup>* mice. CRC, colorectal cancer; NLRP3, NOD-like receptor family, pyrin domain containing 3; IL-1 $\beta$ , interleukin-1 $\beta$ ; TNF- $\alpha$ , tumour necrosis factor- $\alpha$ ; APC, adenomatous polyposis coli; GSK3 $\beta$ , glycogen synthase kinase 3 $\beta$ ; SCFAs, short-chain fatty acids; TCF, T cell factor.

suggest that inflammatory cytokines may directly act on epithelial cells, promote tumour progression and accelerate invasion and metastasis by inducing oxidative stress, producing nitric oxide, colonization of pathogenic bacteria [13,41]. In particular, Tseng *et al* found that the IL-6 signalling pathway could alter the localization of the mismatched repair protein hMSH3, leading to DNA mismatch repair defects and promoting genetic changes in cancer cells [42].

Studies have revealed that some bacterial strains such as *Bacteroides fragilis*, *Clostridium difficile* and *Peptostreptococcus* were enriched in the gut microbiota of CRC patients [43–46]. Moreover, HoIsoi *et al* found that *Peptostreptococcus* interacted with TLR2 and TLR4 on colon cells, induced cholesterol biosynthesis, promoted cell proliferation, and caused dysplasia in mice [47]. In our study, gut microbiota from CRC increased the abundance of *Akkermansia* and *Pseudoflavonifactor*. The abundance of bacteria producing

short-chain fatty acids such as *Ruminococcus*, *Roseburia* and *Clostridium XIIVa* was reduced. The combined action of specific bacteria promotes intestinal inflammation and cancer, and the biofilm formed by bacteria provides shelter for cancer cells [48]. *Clostridium nucleosa* is closely related to CRC and plays a vital role in the occurrence, development, metastasis and prognosis of colorectal cancer. FadA adhesins produced in *clostridium nucleosa* bind to E-cadherin, enhanced the heterotopic expression of  $\beta$ -catenin, and activated Wnt signal pathway to promoted the occurrence of CRC [49]. Recent studies have found that microRNA activated Wnt/ $\beta$ -catenin signalling to promote CRC by inducing tumour cell proliferation, angiogenesis, invasion, and metastasis [31]. In our study, gut microbiota from CRC patients activated Wnt signalling pathway was found by RNA-seq. Our data also showed heterotopic expression of  $\beta$ -catenin, and increased expression of downstream targeted genes in tumour cells, suggesting that gut microbiota of CRC patients could activate Wnt pathway and lead to the progression of adenoma.

The gut microbiota dysbiosis occurs in patients with kinds of bowel diseases such as CRC, Diverticulitis / Diverticulosis, Inflammatory Bowel Disease (IBD), Irritable Bowel Syndrome (IBS), constipation, etc. However, this is not consistent in various diseases of gut microbiota disorder in terms of type, composition, diversity and so on. For example, compared with asymptomatic subjects, the reduction of *Clostridium cluster IV*, *Clostridium cluster IX*, *Fusobacterium* and *Lactobacillaceae* in fecal microbiota was observed in diverticulosis patients. Reduced bacterial diversity and higher instability were observed in IBD patients. The abundance of *Desulfovibrio* and *Bilophila* were increased. Moreover, previously we also reported that fecal microbiota from constipation patients could make intestinal peristalsis slowed down in the antibiotic depletion mice, and the defecation parameters were abnormal. In this study, fecal microbiota transplantation was used to explore the effect of gut microbiota on the progression of adenoma on an overall level. However, whether fecal microbiota from non-CRC patients (such as diverticulitis / diverticulosis) could also induce malignant transformation of intestinal adenoma needs to be further explored. Moreover, specific strains and their metabolites are still unknown and need to be investigated. To sum up, this study found that gut microbiota of CRC patients caused chronic low-grade inflammation, promoted tumour cell proliferation, and inhibited apoptosis, moreover, the disturbed gut microbiota promoted the progression of intestinal adenomas in *Apc<sup>min/+</sup>* mice. Thus, targeted treatment of gut microbiota may become a promising treatment strategy for CRC.

### Funding sources

This study was supported by the grants from the National Natural Science Foundation of China (No. 81741075, No. 81570478, No. 81700456), Tianjin Research Program of Application Foundation and Advanced Technology of China (No.17JCYBJC24900, No.17ZXMFSY00210), China Postdoctoral Science Foundation (No.2019M651049). The funders had no role in study design, data collection, data analysis, interpretation, writing and revision of the manuscript.

### Author contributions

LL, XFL, and WLZ performed experiments together. LL drafted the manuscript; XFL were responsible for donor recruitment and fecal microbiota transplantation; LL and WLZ created figures; WLZ, MY, YS, JHM, TYL, YGC, and XLS analysed data; MQX and HLC conceived the project; WXD and XL contributed to interpretation of the data and revised the manuscript; YL, ZPA, WTL, BMW, KJ, and

HLC directed the research and made the critical revision. All authors identified the manuscript and finally approved the article.

### Declaration of Competing Interest

The authors declare no conflicts of interest.

### Acknowledgements

We thank the National Natural Science Foundation of China, Tianjin Research Program of Application Foundation and Advanced Technology of China and China Postdoctoral Science Foundation for their financial support. The funders had no role in study design, data collection, data analysis, interpretation, writing and revision of the manuscript.

### References

- Bray F, Ferlay J, Soerjomataram I, Siegel RL, Torre LA, Jemal A. Global cancer statistics 2018: GLOBOCAN estimates of incidence and mortality worldwide for 36 cancers in 185 countries. *CA Cancer J Clin* 2018;68(6):394–424.
- Lucas C, Barnich N, Microbiota HTTN. Inflammation and colorectal cancer. *Int J Mol Sci* 2017;18:6.
- Kerr J, Anderson C, Lippman SM. Physical activity, sedentary behaviour, diet, and cancer: an update and emerging new evidence. *Lancet Oncol* 2017;18(8):e457–71.
- Yang J, Yu J. The association of diet, gut microbiota and colorectal cancer: what we eat may imply what we get. *Protein Cell* 2018;9(5):474–87.
- Beaugerie L, Itzkowitz SH. Cancers complicating inflammatory bowel disease. *N Engl J Med* 2015;372(15):1441–52.
- Jia W, Xie G, Jia W. Bile acid-microbiota crosstalk in gastrointestinal inflammation and carcinogenesis. *Nat Rev Gastroenterol Hepatol* 2018;15(2):111–28.
- O’Keefe SJ. Diet, microorganisms and their metabolites, and colon cancer. *Nat Rev Gastroenterol Hepatol* 2016;13(12):691–706.
- Chakradhar S. Colorectal cancer: 5 big questions. *Nature*. 2015;521(7551):S16.
- Gao R, Gao Z, Huang L, Qin H. Gut microbiota and colorectal cancer. *Eur J Clin Microbiol Infect Dis* 2017;36(5):757–69.
- Lynch SV, Pedersen O. The human intestinal microbiome in health and disease. *N Engl J Med* 2016;375(24):2369–79.
- Blander JM, Longman RS, Iliev ID, Sonnenberg GF, Artis D. Regulation of inflammation by microbiota interactions with the host. *Nat Immunol* 2017;18(8):851–60.
- Coker OO, Nakatsu G, Dai RZ, et al. Enteric fungal microbiota dysbiosis and ecological alterations in colorectal cancer. *Gut*. 2019;68(4):654–62.
- Kang M, Martin A. Microbiome and colorectal cancer: unraveling host-microbiota interactions in colitis-associated colorectal cancer development. *Semin Immunol* 2017;32:3–13.
- Yu J, Feng Q, Wong SH, et al. Metagenomic analysis of faecal microbiome as a tool towards targeted non-invasive biomarkers for colorectal cancer. *Gut*. 2017;66(1):70–8.
- Raskov H, Burcharth J, Pommergaard HC. Linking gut microbiota to colorectal cancer. *J Cancer* 2017;8(17):3378–95.
- Yu T, Guo F, Yu Y, et al. *Fusobacterium nucleatum* promotes chemoresistance to colorectal cancer by modulating autophagy. *Cell*. 2017;170(3):548–563.e16.
- HLP T, Nobrega FL, van der Oost J, de Vos WM. Bowel biofilms: tipping points between a healthy and compromised gut. *Trends Microbiol* 2019;27(1):17–25.
- Arkan MC. The intricate connection between diet, microbiota, and cancer: a jigsaw puzzle. *Semin Immunol* 2017;32:35–42.
- Meng C, Bai C, Brown TD, Hood LE, Tian Q. Human gut microbiota and gastrointestinal cancer. *Genomics Proteomics Bioinformatics* 2018;16(1):33–49.
- Gopalakrishnan V, Helmink BA, Spencer CN, Reuben A, Wargo JA. The influence of the gut microbiome on cancer, immunity, and cancer immunotherapy. *Cancer Cell* 2018;33(4):570–80.
- Chen J, Pitmon E, Wang K. Microbiome, inflammation and colorectal cancer. *Semin Immunol* 2017;32:43–53.
- Wong SH, Zhao L, Zhang X, et al. Gavage of fecal samples from patients with colorectal cancer promotes intestinal carcinogenesis in germ-free and conventional mice. *Gastroenterology*. 2017;153(6):1621–1633.e6.
- Zhang L, Shay JW. Multiple roles of APC and its therapeutic implications in colorectal cancer. *J Natl Cancer Inst* 2017;109(8).
- Kelly CR, Kahn S, Kashyap P, et al. Update on fecal microbiota transplantation 2015: indications, methodologies, mechanisms, and outlook. *Gastroenterology*. 2015;149(1):223–37.
- Le RT, Llopis M, Lepage P, et al. Intestinal microbiota determines development of non-alcoholic fatty liver disease in mice. *Gut*. 2013;62(12):1787–94.
- Zheng P, Zeng B, Zhou C, et al. Gut microbiome remodeling induces depressive-like behaviors through a pathway mediated by the host’s metabolism. *Mol Psychiatry* 2016;21(6):786–96.
- Khanna S, Vazquez-Baeza Y, González A, et al. Changes in microbial ecology after fecal microbiota transplantation for recurrent *C. difficile* infection affected by underlying inflammatory bowel disease. *Microbiome*. 2017;5(1):55.

- [28] JAK M, Mullish BH, Pechlivanis A, et al. Inhibiting growth of clostridioides difficile by restoring valerate, produced by the intestinal microbiota. *Gastroenterology*. 2018;155(5):1495–1507.e15.
- [29] Schuijt TJ, Lankelma JM, Scicluna BP, et al. The gut microbiota plays a protective role in the host defence against pneumococcal pneumonia. *Gut*. 2016;65(4):575–83.
- [30] Cao H, Xu M, Dong W, et al. Secondary bile acid-induced dysbiosis promotes intestinal carcinogenesis. *Int J Cancer* 2017;140(11):2545–56.
- [31] Rahmani F, Avan A, Hashemy SI, Hassanian SM. Role of Wnt/ $\beta$ -catenin signaling regulatory microRNAs in the pathogenesis of colorectal cancer. *J Cell Physiol* 2018;233(2):811–17.
- [32] Arthur JC, Perez-Chanona E, Mühlbauer M, et al. Intestinal inflammation targets cancer-inducing activity of the microbiota. *Science*. 2012;338(6103):120–3.
- [33] Macia L, Tan J, Vieira AT, et al. Metabolite-sensing receptors GPR43 and GPR109A facilitate dietary fibre-induced gut homeostasis through regulation of the inflammasome. *Nat Commun* 2015;6:6734.
- [34] Zhao Y, Chen F, Wu W, et al. GPR43 mediates microbiota metabolite SCFA regulation of antimicrobial peptide expression in intestinal epithelial cells via activation of mTOR and STAT3. *Mucosal Immunol* 2018;11(3):752–62.
- [35] Hale VL, Jeraldo P, Chen J, et al. Distinct microbes, metabolites, and ecologies define the microbiome in deficient and proficient mismatch repair colorectal cancers. *Genome Med* 2018;10(1):78.
- [36] Burns MB, Montassier E, Abrahante J, et al. Colorectal cancer mutational profiles correlate with defined microbial communities in the tumor microenvironment. *PLoS Genet* 2018;14(6):e1007376.
- [37] Bartley AN, Yao H, Barkoh BA, et al. Complex patterns of altered MicroRNA expression during the adenoma-adenocarcinoma sequence for microsatellite-stable colorectal cancer. *Clin Cancer Res* 2011;17(23):7283–93.
- [38] Coleman OI, Haller D. Bacterial signaling at the intestinal epithelial interface in inflammation and cancer. *Front Immunol* 2017;8:1927.
- [39] van Itallie CM, Anderson JM. Architecture of tight junctions and principles of molecular composition. *Semin Cell Dev Biol* 2014;36:157–65.
- [40] Zeineldin M, Neufeld KL. Understanding phenotypic variation in rodent models with germline Apc mutations. *Cancer Res* 2013;73(8):2389–99.
- [41] Brennan CA, Garrett WS. Gut microbiota, inflammation, and colorectal cancer. *Annu Rev Microbiol* 2016;70:395–411.
- [42] Tseng-Rogenski SS, Hamaya Y, Choi DY, Carethers JM. Interleukin 6 alters localization of hMSH3, leading to DNA mismatch repair defects in colorectal cancer cells. *Gastroenterology*. 2015;148(3):579–89.
- [43] Brennan CA, Garrett WS. *Fusobacterium nucleatum* - symbiont, opportunist and oncobacterium. *Nat Rev Microbiol* 2019;17(3):156–66.
- [44] Komiya Y, Shimomura Y, Higurashi T, et al. Patients with colorectal cancer have identical strains of *Fusobacterium nucleatum* in their colorectal cancer and oral cavity. *Gut*. 2019;68(7):1335–7.
- [45] Flemer B, Warren RD, Barrett MP, et al. The oral microbiota in colorectal cancer is distinctive and predictive. *Gut*. 2018;67(8):1454–63.
- [46] Fukugaiti MH, Ignacio A, Fernandes MR, et al. High occurrence of *Fusobacterium nucleatum* and *Clostridium difficile* in the intestinal microbiota of colorectal carcinoma patients. *Braz J Microbiol* 2015;46(4):1135–1140.
- [47] Tsoi H, ESH C, Zhang X, et al. *Peptostreptococcus anaerobius* induces intracellular cholesterol biosynthesis in colon cells to induce proliferation and causes dysplasia in mice. *Gastroenterology*. 2017;152(6):1419–1433.e5.
- [48] Dejea CM, Fathi P, Craig JM, et al. Patients with familial adenomatous polyposis harbor colonic biofilms containing tumorigenic bacteria. *Science*. 2018;359(6375):592–7.
- [49] Rubinstein MR, Wang X, Liu W, Hao Y, Cai G, Han YW. *Fusobacterium nucleatum* promotes colorectal carcinogenesis by modulating E-cadherin/ $\beta$ -catenin signaling via its FadA adhesin. *Cell Host Microbe* 2013;14(2):195–206.